



Proceeding Paper

# Directed Evolution of a Genetically Encoded Bioluminescent $\text{Ca}^{2+}$ Sensor †

Yufeng Zhao <sup>1</sup>, Sungmo Lee <sup>1</sup>, Robert E. Campbell <sup>2,3</sup>  and Michael Z. Lin <sup>1,4,5,\*</sup> 

<sup>1</sup> Department of Neurobiology, Stanford University, Stanford, CA 94305, USA; yufengz@stanford.edu (Y.Z.); smoolee@stanford.edu (S.L.)

<sup>2</sup> Department of Chemistry, The University of Tokyo, Tokyo 113-0033, Japan; campbell@chem.s.u-tokyo.ac.jp

<sup>3</sup> Department of Chemistry, University of Alberta, Edmonton, AB T6G 2G2, Canada

<sup>4</sup> Department of Bioengineering, Stanford University, Stanford, CA 94305, USA

<sup>5</sup> Department of Chemical and Systems Biology, Stanford University, Stanford, CA 94305, USA

\* Correspondence: mzlin@stanford.edu

† Presented at the 3rd International Electronic Conference on Biosensors, 8–21 May 2023; Available online: <https://iecb2023.sciforum.net/>.

**Abstract:** The use of genetically encoded fluorescent sensors for the calcium ion ( $\text{Ca}^{2+}$ ) has revolutionized neuroscience research by allowing for the recording of dozens of neurons at the single-cell level in living animals. However, fluorescence imaging has some limitations such as the need for excitation light, which can result in a highly auto-fluorescent background and phototoxicity. In contrast, bioluminescent sensors using luciferase do not require excitation light, making them ideal for non-invasive deep tissue imaging in mammals. Our lab has previously developed a bioluminescent  $\text{Ca}^{2+}$  sensor CaMBI to image  $\text{Ca}^{2+}$  activity in the mouse liver, but its responsiveness to  $\text{Ca}^{2+}$  changes was suboptimal. To improve the performance of this sensor, we applied directed evolution to screen for genetic variants with increased responsiveness. Through several rounds of evolution, we identified variants with more than five times improved responsiveness in vitro. We characterized the improved sensors in culture cell lines and dissociated rat neurons and confirmed that they exhibited a higher sensitivity to changes in intracellular  $\text{Ca}^{2+}$  levels compared to their progenitor. These optimized  $\text{Ca}^{2+}$  sensors have the potential for non-invasive imaging of  $\text{Ca}^{2+}$  activity in vivo, particularly in the brain.

**Keywords:**  $\text{Ca}^{2+}$  sensor; directed evolution; bioluminescence



**Citation:** Zhao, Y.; Lee, S.; Campbell, R.E.; Lin, M.Z. Directed Evolution of a Genetically Encoded Bioluminescent  $\text{Ca}^{2+}$  Sensor. *Eng. Proc.* **2023**, *35*, 20. <https://doi.org/10.3390/IECB2023-14563>

Academic Editor: Sara Tombelli

Published: 8 May 2023



**Copyright:** © 2023 by the authors. Licensee MDPI, Basel, Switzerland. This article is an open access article distributed under the terms and conditions of the Creative Commons Attribution (CC BY) license (<https://creativecommons.org/licenses/by/4.0/>).

## 1. Introduction

Genetically encoded fluorescent sensors for the calcium ion ( $\text{Ca}^{2+}$ ) have revolutionized neuroscience research by enabling the recording of dozens of neurons at the single-cell level in living animals [1,2]. However, fluorescence imaging has drawbacks, including the requirement for excitation light, which can result in a highly auto-fluorescent background and phototoxicity. In contrast, bioluminescent sensors that use luciferase do not need excitation light, making them well-suited for non-invasive deep tissue imaging in mammals.

Although a number of bioluminescent  $\text{Ca}^{2+}$  sensors have been developed, most of these sensors, including CaMBI [3], BRIC [4], GeNL( $\text{Ca}^{2+}$ ) [5], and CalFluxVTN [6], suffer from limited dynamic range (response to  $\text{Ca}^{2+}$  changes), with less than  $10\times$  response when switching from a  $\text{Ca}^{2+}$ -apo to a  $\text{Ca}^{2+}$ -bound state in vitro compared to the over  $50\times$  change in fluorescent GCaMP sensors. Farhana et al. leveraged the large dynamic range of GCaMP and engineered a sensitive bioluminescent/fluorescent bimodal  $\text{Ca}^{2+}$  sensor GLICO [7]. They inserted GCaMP6 into NanoBit, resulting in a dynamic range of  $23\times$ , but GLICO only produced  $\sim 10\%$  of the molecular brightness of their previously developed sensor GeNL( $\text{Ca}^{2+}$ ), and a negligible portion of red photons, resulting in unfavored performance in deep tissue imaging.

We previously developed a  $\text{Ca}^{2+}$  sensor, orange CaMBI (orange calcium-modulated bioluminescent indicator) [3], with substantial red photons  $>600$  nm through resonance energy transfer from the NanoLuc domain to the two copies of CyOFP to enable deep tissue  $\text{Ca}^{2+}$  imaging (Figure 1a). Recently, we reported the novel substrate cephalofurimazine (CFz) with enhanced blood–brain barrier permeability for NanoLuc and its derived sensors, including those of the CaMBI series [8].  $\text{Ca}^{2+}$  signals were successfully detected in the brain of a CaMBI-transgenic mouse. However, hemodynamic changes in the brain caused interfering bioluminescent signal changes as NanoLuc-based bioluminescence requires oxygen. To further strengthen bioluminescence  $\text{Ca}^{2+}$  imaging, efforts should be made to improve the sensitivity of  $\text{Ca}^{2+}$  sensors such that  $\text{Ca}^{2+}$ -dependent signals are predominant in the imaging. While directed evolution has been successful in the optimization of the performance of fluorescent  $\text{Ca}^{2+}$  sensors, little effort has been made to improve bioluminescent  $\text{Ca}^{2+}$  sensors with this strategy. Here, we report the development of several new CaMBI variants with improved brightness and dynamic range using protein engineering techniques such as directed evolution. We characterized the improved sensors in culture cell lines and dissociated rat neurons and confirmed that they exhibited a higher sensitivity to changes in intracellular  $\text{Ca}^{2+}$  levels compared to their progenitor.

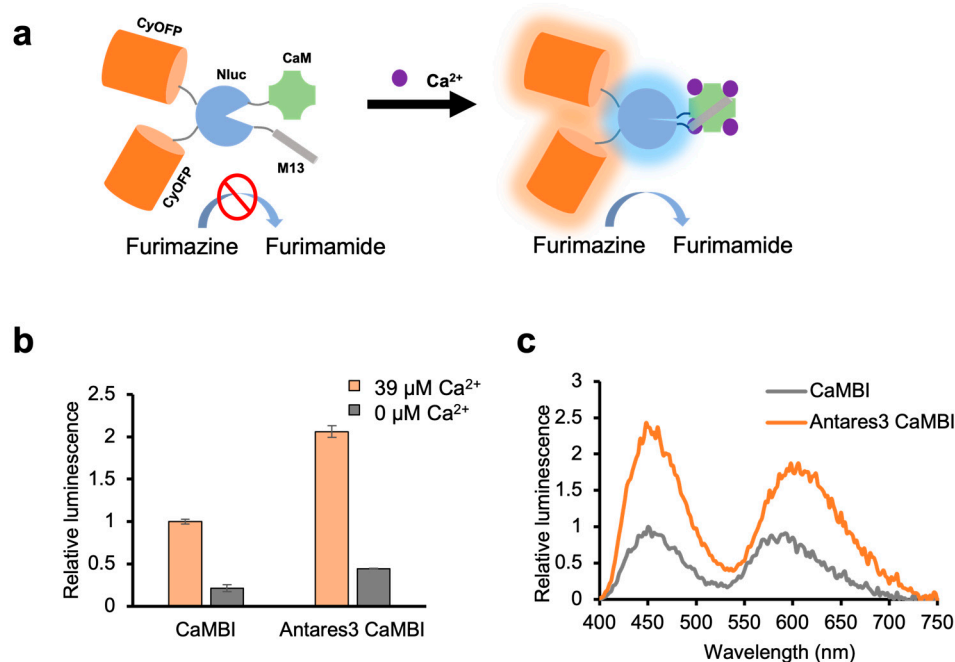


**Figure 1.** (a) Schematic representation of CaMBI. (b) Relative total luminescence of CaMBI and Antares3 CaMBI in the presence and absence of  $\text{Ca}^{2+}$ . (c) Luminescence spectra of CaMBI and Antares3 CaMBI. (Error bars represent s.d.).

## 2. Methods

### 2.1. Directed Evolution of CaMBI

The libraries of CaMBI were generated using an error prone PCR reaction using the GeneMorph II Random Mutagenesis Kit (Agilent). PCR products were purified via agarose gel electrophoresis and then cloned into the pBAD vectors using the In-Fusion Cloning Kit (Takara). The assembled constructs were then transformed into electrocompetent *E. coli* cells to express the library, which were plated on LB-agar plates supplemented with 400  $\mu\text{g}/\text{mL}$  ampicillin and 0.02% (wt/vol) arabinose for overnight culture at 37 °C. On the following day, colonies were randomly selected for subsequent inoculation in 96-well plates with liquid LB medium containing ampicillin and arabinose for 18 h in a 37 °C shaking incubator. The cells were collected by centrifugation and lysed using B-PER (Thermo Scientific, Waltham, MA, USA). The supernatant of each well was diluted into 1  $\times$  Tris buffered saline (TBS), with 10 mM EGTA (0  $\mu\text{M}$   $\text{Ca}^{2+}$ ) or 10 mM EGTA-Ca (39  $\mu\text{M}$

Ca<sup>2+</sup>). Luciferase substrate CFz was added to reach a final concentration of 25 μM for the luminescence measurement of the CaMBI variant in a microplate reader. The luminescence signals of each variant in 0 or 39 μM Ca<sup>2+</sup> were used for calculation, and plasmids of the variants exhibiting the largest signal contrast were recovered for sequencing and were used for the next round of mutagenesis.

## 2.2. *In Vitro* Characterization

CaMBI variants were cloned into pcDNA vectors for expression in mammalian cells. Assembled constructs were transfected into HEK293A cells using Lipofectamine 3000 Transfection Reagent (Invitrogen, Waltham, MA, USA) according to the manufacturer's protocol. Cells were seeded in a 24-well plate and maintained in high-glucose Dulbecco's Modified Eagle Medium (DMEM, Life Technologies, Carlsbad, CA, USA) with 5% FBS at 37 °C in a humidified CO<sub>2</sub> incubator. Then, 24 h after transfection, the medium was removed by vacuum and the cells were lysed with Passive Lysis Buffer (Promega, Madison, WI, USA). The cell lysates were diluted into TBS buffer with 0, 146 nM, or 39 μM Ca<sup>2+</sup> and the substrate CFz was added to the buffer for luminescence measurement in a microplate reader.

## 2.3. *HeLa* Cell Culture and Imaging

HeLa cells were maintained and transfected using the same protocol as HEK293A cells (described above). Cells expressing CaMBI variants were imaged 24 or 48 h after transfection. Prior to imaging, the cell medium was replaced with HEPES buffered HBSS with 25 μM CFz substrate. Cells were imaged using a Zeiss Axiovert 200M fluorescence microscope with a 40 × 1.2-NA C-Apochromat water-immersion objective and an ORCA-Flash4.0 V2 C11440-22CU scientific CMOS camera. The microscope was controlled using MicroManager. No light source or optical filter was used for luminescence imaging. To image the fluorescence signals of CaMBI, a metal-halide arc lamp (Exfo) was used as the excitation light source with a 545RDF10 excitation filter and fluorescence was collected in a 565ALP emission filter. Time-lapse images were recorded every 5 s with 4 × 4 binning and 2 s exposure time. Histamine was added to the imaging buffer to reach a final concentration of 10 μM, approximately 1 min after the recording began.

## 2.4. Culture and Imaging of Dissociated Neurons

Dissociated rat neurons were generated according to the protocol described previously [9]. Briefly, the neurons were plated in a 24-well plate in Neurobasal media with 10% FBS, 2 mM GlutaMAX, and B27 supplement. On days-in-vitro (DIV) 1, a half of the media was changed so that the FBS can be reduced to 1% for each well. Then, a half of the media was replaced every 3 days with fresh Neurobasal media without FBS. Neurons were transfected at 9–11 DIV using Lipofectamine 2000 (Life Technologies). The imaging buffer and microscopic setup were similar to those described in Section 2.3. Time-lapse images were recorded at 10 Hz with a 0.1 s exposure time. HHBSS buffer with 50 μM KCl was 1:1 added to the cell imaging buffer to reach a final concentration of 25 μM KCl to depolarize neurons during the imaging.

## 3. Results and Discussion

In order to enhance the luminescence signals of CaMBI, we began by introducing mutations to the CyOFP and NanoLuc domains. These domains had previously been optimized in our efforts to improve Antares, which served as the basis for engineering CaMBI. The resulting mutations led to an increase in CaMBI's expression levels in mammalian cells, as well as a moderate improvement in its catalytic activity against the substrate CFz. The new variant is designated as Antares3 CaMBI. Importantly, these improvements did not compromise CaMBI's ability to sense Ca<sup>2+</sup> (Figure 1b,c).

Our next goal was to improve the dynamic range of CaMBI by introducing mutations to the NanoLuc and Ca<sup>2+</sup> sensing domains. We reasoned that mutations in the NanoLuc

and  $\text{Ca}^{2+}$  sensing domains could potentially improve the dynamic range of CaMBI. We used directed evolution and applied random mutagenesis to these domains. In each round, we screened 400–600 randomly selected variants for their luminescence at 0 and  $39 \mu\text{M}$   $\text{Ca}^{2+}$ , and sequenced the variants with the best performance to use as templates for the next round (Figure 2).

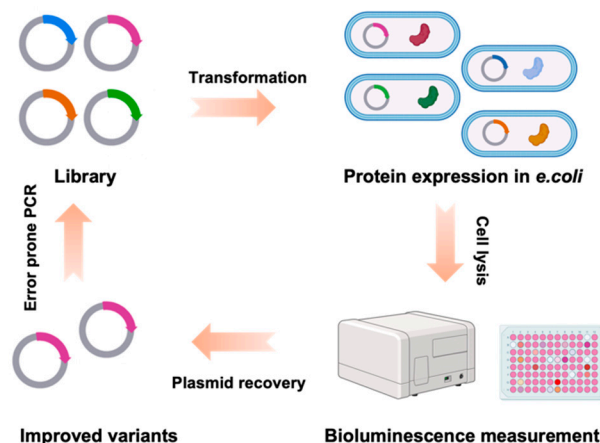


**Figure 2.** Directed evolution of CaMBI.

After three rounds of directed evolution, we obtained a variant named L3-P2C9 with eight mutations in total (two in the NanoLuc domain and six in the  $\text{Ca}^{2+}$  sensing domain), which demonstrated approximately 5-fold enhanced dynamic range compared to the original template Antares3 CaMBI (Figure 3a). To eliminate unnecessary mutations in the course of directed evolution, we performed single mutation reversion and measured the dynamic range of each variant. We also introduced a beneficial mutation discovered during directed evolution that did not exist in L3-P2C9. As a result, we obtained two new variants termed L3-P2C9.1 (one beneficial mutation and one reversed mutation relative to L3-P2C9) and L3-P2C9.2 (one beneficial mutation and two reversed mutations relative to L3-P2C9). The characterization of these sensors in lysed mammalian cells confirmed the enhanced dynamic range, with L3-P2C9.1 exhibiting the largest dynamic range but lower cellular brightness (Figure 3a), and with L3-P2C9.2 having a slightly higher apparent affinity to  $\text{Ca}^{2+}$  than the others (Figure 3c). Analogous luminescent spectra suggest that cumulative mutations after directed evolution have little impact on the bioluminescent resonance energy transfer efficiency (Figure 3b). Overall, our approach of directed evolution successfully improved the dynamic range of CaMBI through random mutations in the NanoLuc and  $\text{Ca}^{2+}$  sensing domains.

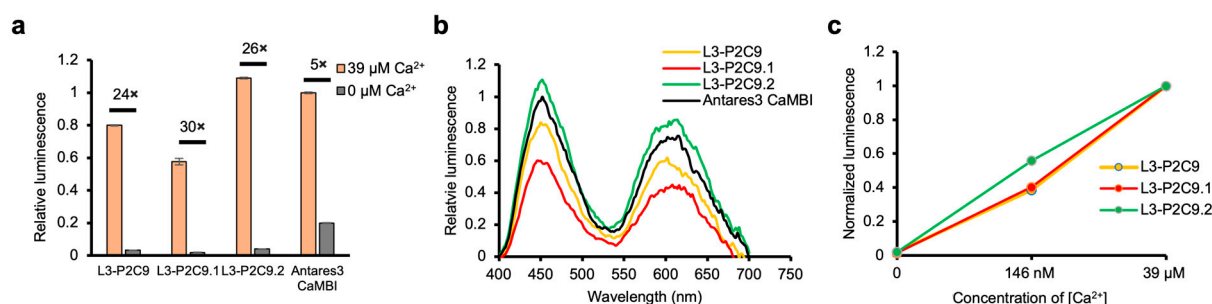


**Figure 3.** (a) Relative total luminescence of new CaMBI variants and Antares3 CaMBI in the presence and absence of  $\text{Ca}^{2+}$ . (b) Luminescence spectra of CaMBI variants. (c) Luminescence of CaMBI variants at 0, 146 nM, or  $39 \mu\text{M}$   $\text{Ca}^{2+}$ . (Error bars represent s.d.).

We next evaluated the performance of  $\text{Ca}^{2+}$  sensors by comparing their response to histamine-induced intracellular  $\text{Ca}^{2+}$  oscillation in cultured cells, a commonly used assay to

characterize fluorescent  $\text{Ca}^{2+}$  sensors. We expressed CaMBI variants in HeLa cells through transient transfection (Figure 4a) and recorded luminescence responses upon histamine stimulation (Figure 4b). The first  $\text{Ca}^{2+}$  wave was used to evaluate the performance of the sensors. All three improved CaMBI variants demonstrated higher responses than the original CaMBI, while negligible differences were observed among the three new variants (Figure 4c).

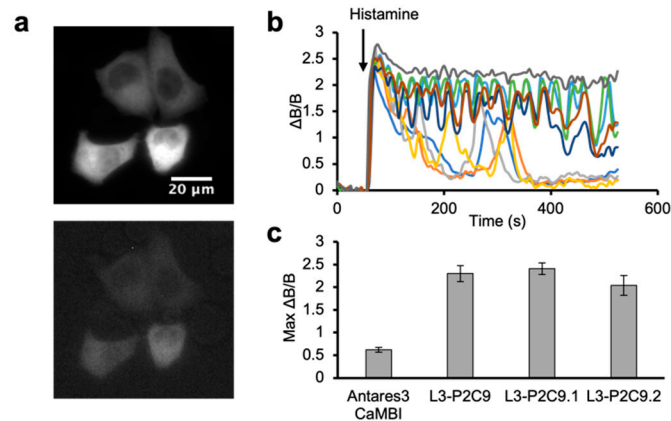


**Figure 4.** (a) Representative fluorescence (**upper**) and luminescence (**lower**) microscopic image of L3-P2C9. (b) Representative time-lapsed luminescence signals of individual cells upon histamine stimulation (indicated by the arrow). Each trace represents the luminescence signal of a single cell. (c) Responses of CaMBI variants to histamine stimulation. (Error bars represent s.e.m.).

To assess the sensitivity of the CaMBI variants in neurons, we expressed the variants in cultured dissociated rat neurons (Figure 5a) and recorded their response to elevated  $\text{Ca}^{2+}$  levels upon KCl-induced neuronal depolarization (Figure 5b). Among all the variants examined, L3-P2C9 demonstrated the largest responses, showing a 2-fold better  $\Delta\text{B}/\text{B}$  compared to the original CaMBI (Figure 5c).

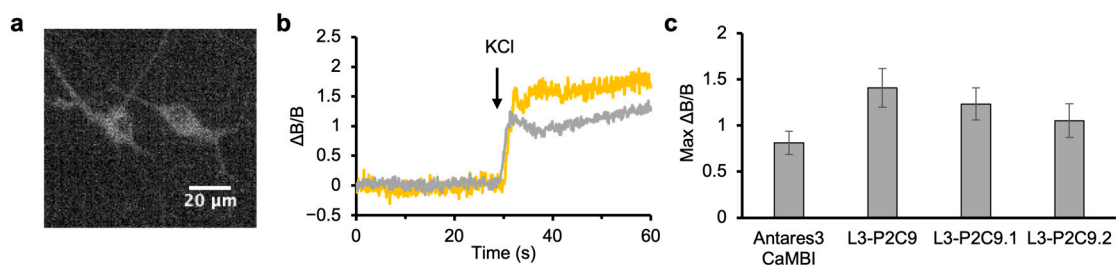


**Figure 5.** (a) Representative luminescence microscopic image of L3-P2C9. (b) Representative time-lapsed luminescence signals of individual neurons upon KCl-induced depolarization (indicated by the arrow). (c) Responses of CaMBI variants to  $\text{Ca}^{2+}$  elevation upon KCl-induced depolarization. (Error bars represent s.e.m.).

#### 4. Conclusions

We have improved the responsiveness of a bioluminescent  $\text{Ca}^{2+}$  sensor CaMBI through directed evolution. The optimized variants demonstrated significantly higher responses to  $\text{Ca}^{2+}$  changes in the cultured mammalian cell line and dissociated rat neurons.

**Author Contributions:** Conceptualization, Y.Z. and M.Z.L.; methodology, Y.Z. and S.L.; writing, Y.Z. and M.Z.L.; supervision, M.Z.L. and R.E.C.; funding acquisition, M.Z.L. and R.E.C. All authors have read and agreed to the published version of the manuscript.

**Funding:** Funding in the lab of M.Z.L. was provided by NIH grants R21NS122055 and 1R21DA048252. Work in the lab of R.E.C. was supported by the Canadian Institutes of Health Research (CIHR, FS-154310) and the Natural Sciences and Engineering Research Council of Canada (NSERC, RGPIN 2018-04364). Y.Z. was a recipient of the Stanford University School of Medicine Dean's Postdoctoral Fellowship.

**Institutional Review Board Statement:** The animal study protocols were approved by the Stanford Institutional Animal Use and Care Committee.

**Informed Consent Statement:** Not applicable.

**Data Availability Statement:** The data are available in the article and available on request.

**Acknowledgments:** The authors thank Gareth Lambkin (Department of Chemistry, University of Alberta) for his technical assistance.

**Conflicts of Interest:** The authors declare no conflict of interest.

## References

1. Chen, T.W.; Wardill, T.J.; Sun, Y.; Pulver, S.R.; Renninger, S.L.; Baohan, A.; Schreiter, E.R.; Kerr, R.A.; Orger, M.B.; Jayaraman, V.; et al. Ultrasensitive fluorescent proteins for imaging neuronal activity. *Nature* **2013**, *499*, 295–300. [[CrossRef](#)] [[PubMed](#)]
2. Dana, H.; Sun, Y.; Mohar, B.; Hulse, B.K.; Kerlin, A.M.; Hasseman, J.P.; Tsegaye, G.; Tsang, A.; Wong, A.; Patel, R.; et al. High-performance calcium sensors for imaging activity in neuronal populations and microcompartments. *Nat. Methods* **2019**, *16*, 649–657. [[CrossRef](#)] [[PubMed](#)]
3. Oh, Y.; Park, Y.; Cho, J.; Wu, H.; Paulk, N.K.; Liu, L.X.; Kim, N.; Kay, M.A.; Wu, J.C.; Lin, M.Z. An orange calcium-modulated bioluminescent indicator for non-invasive activity imaging. *Nat. Chem. Biol.* **2019**, *15*, 433–436. [[CrossRef](#)] [[PubMed](#)]
4. Tian, X.; Zhang, Y.; Li, X.; Xiong, Y.; Wu, T.; Ai, H.W. A luciferase prosubstrate and a red bioluminescent calcium indicator for imaging neuronal activity in mice. *Nat. Commun.* **2022**, *13*, 3967. [[CrossRef](#)] [[PubMed](#)]
5. Suzuki, K.; Kimura, T.; Shinoda, H.; Bai, G.; Daniels, M.J.; Arai, Y.; Nakano, M.; Nagai, T. Five colour variants of bright luminescent protein for real-time multicolour bioimaging. *Nat. Commun.* **2016**, *7*, 13718. [[CrossRef](#)] [[PubMed](#)]
6. Yang, J.; Cumberbatch, D.; Centanni, S.; Shi, S.-Q.; Winder, D.; Webb, D.; Johnson, C.H. Coupling optogenetic stimulation with NanoLuc-based luminescence (BRET) Ca<sup>++</sup> sensing. *Nat. Commun.* **2016**, *7*, 13268. [[CrossRef](#)] [[PubMed](#)]
7. Farhana, I.; Hossain, M.N.; Suzuki, K.; Matsuda, T.; Nagai, T. Genetically encoded fluorescence/bioluminescence bimodal indicators for Ca<sup>2+</sup> imaging. *ACS Sens.* **2019**, *4*, 1825–1834. [[CrossRef](#)] [[PubMed](#)]
8. Su, Y.; Walker, J.R.; Hall, M.P.; Klein, M.A.; Wu, X.; Encell, L.P.; Casey, K.M.; Liu, L.X.; Hong, G.; Lin, M.Z.; et al. An optimized bioluminescent substrate for non-invasive imaging in the brain. *Nat. Chem. Biol.* **2023**, 1–9. [[CrossRef](#)] [[PubMed](#)]
9. Villette, V.; Chavarha, M.; Dimov, I.K.; Bradley, J.; Pradhan, L.; Mathieu, B.; Evans, S.W.; Chamberland, S.; Shi, D.; Yang, R.; et al. Ultrafast Two-Photon Imaging of a High-Gain Voltage Indicator in Awake Behaving Mice. *Cell* **2019**, *179*, 1590–1608.e23. [[CrossRef](#)] [[PubMed](#)]

**Disclaimer/Publisher's Note:** The statements, opinions and data contained in all publications are solely those of the individual author(s) and contributor(s) and not of MDPI and/or the editor(s). MDPI and/or the editor(s) disclaim responsibility for any injury to people or property resulting from any ideas, methods, instructions or products referred to in the content.